Supporting information

A Highly Efficient FeP/CeO_2-NF Hybrid Electrode for the Oxygen Evolution Reaction

Jian Liu,[a] Yan Gao, [a,b*] Yu Wei,[a] Xuyang Chen,[a] Shengjie Hao,[a] Xin Ding,[a,c*] and Lijun Pand [d*]

[a]State Key Laboratory of Fine Chemicals, DUT-KTH Joint Education and Research Center on Molecular Devices, Dalian University of Technology (DUT), Dalian 116024, P. R. China.
[b]Ningbo Institute of Dalian University of Technology, Ningbo, 315000, P. R.China
[c]College of Chemistry and Chemical Engineering, Qingdao University, Qingdao 266071, Shandong, P. R. China.
[d]Department of Environmental Health Protection, National Institute for Environmental Health, Chinese Center for Disease Control and Prevention, No.7 Nanli, Panjiayuan, Beijing, 100021, P. R. China.
* Corresponding author
E-mail addresses: dr.gaoyan@dlut.edu.cn (Y. Gao*); dingxin@qdu.edu.cn (X. Ding*); panlijun@nieh.chinacdc.cn (L. Pan*)

Experimental section:

Chemicals and materials

The materials in the experiment were used directly without any purification: Cerium (III) nitrate hexahydrate ($Ce(NO_3)\cdot 6H_2O$，Sinopharm Chemical Reagent CO., Ltd, 99.0%), Iron(III) nitrate nonahydrate ($Fe(NO_3)_3\cdot 9H_2O$, Sinopharm Chemical Reagent CO., Ltd, 98.5%), Ammonium oxalate ($(NH_4)_2C_2O_4\cdot H_2O$, Tianjing Damao Chemical Reagent CO., Ltd, 99.8%), Sodium chloride (NaCl, Tianjing Damao Chemical Reagent CO., Ltd, 99.5%), Potassium hydroxide (KOH, Aladdin Chemical Reagent CO., Ltd, 95%), Ni foam (1 cm×2 cm, thickness 1.5 mm, bulk density 200 mg/cm^2) was purchased from Suzhou jiashide metal foam Co., Ltd.

Fabrication of FeP/CeO_2-NF, FeP-NF and CeO_2-NF electrodes

Firstly, NF (1 cm×2 cm) was washed by dilute HCl, ethanol and deionized water each 30 minutes to get rid of the surface oxide and pollutants, and dried in the air for subsequent use. In a typical procedure,first, CeO_2 was electrodeposited on the NF in a solution containing 2 mM $Ce(NO_3)_3$, 10 mM NaCl at 70 ℃ under the current density of 0.25 mA/cm^2 for 10 min. Second, FeOOH particles were electrodeposited on the CeO_2-NF electrode in a solution containing 1 mM $Fe(NO_3)_3$, 2.5 mM $(NH_4)_2C_2O_4$, 2 mM NaCl at 50℃

under the current density of 0.2 mA/cm^2 for 10 min. Then the electrodes were washed by deionized water, and dried in the air. After that, the FeOOH/CeO_2-NF electrodes and NaH_2PO_2 were put in a porcelain boat and calcinated for 2 h at 350°C in a flowing Ar atmosphere. Finally, the FeP/CeO_2-NF electrode was obtained. The FeP-NF electrode was prepared in the same way without CeO_2.

Material characterization

X-ray diffraction (XRD) measurements were collected by a D/max-2400 diffractometer. The measurement was performed from 10° to 80° and the scanning speed was 10 degrees per minute. The microstructure and morphology of synthesized materials were observed by Nova NanoSEM 450 equipment. The energy-dispersion X-ray (EDX) spectrum analysis and elemental distributions mapping were obtained by using the energy-dispersion X-ray fluorescence analyzer. Transmission electron microscopy (TEM) and high-resolution transmission electron microscopy (HRTEM) was received by using FEI TF30. The X-ray photoelectron spectroscopy (XPS) images were recorded by a Thermo ESCALAB XI+. And the binding energy was calibrated according to C 1s (284.8 eV).

Electrochemical characterization

All the electrochemical characterization was performed by a computer-controlled electrochemical workstation (CHI 660E Shanghai Chenhua Instrument Co.,Ltd) at room temperature. In a three-electrode system: A previously prepared electrode was used as the working electrode, a Pt net (1×1 cm) was used as the counter electrode and a HgO/Hg electrode was used as the reference electrode. The reference electrode was calibrated with $Ru(bpy)_3$ before using. 1M Potassium hydroxide (KOH) solution was used as the electrolyte solution. The potential obtained by the test was converted to reversible hydrogen electrode (RHE)：$E_{RHE}=E_{HgO/Hg}+0.0591$ pH+0.098 V. The working electrode was activated by performing an electrochemical test of 40 CV scans, which voltage was between 1.1 V and 1.6 V and the scan rate was 20 mv/s. Linear sweep voltammetry (LSV) measurements were performed at a scanning speed at 5 mv/s in 1 M

KOH solution with 90% iR compensation. Long-term stability measurements were obtained by chronopotentiometry experiments at a constant current density of 10 mA/cm^2 without iR compensation. Tafel curves were derived from Linear sweep voltammetry (with 90% iR compensation) by plotting overpotential η against log(J). Electrochemical impedance spectroscopy experiments were tested in 1.0 M KOH solution at 1.5 V vs. RHE with the frequency ranged from 10^{-2} to 10^5 Hz. Double-layer capacitance (C_{dl}) was obtained by measuring CV curves at different scanning speeds (10-100 mV/s) in the non-faraday region (1.03-1.13 V vs. RHE). Electrochemical active surface area (ECSA) was determined based on the double-layer capacitance (C_{dl}) by measuring the CV curves of the electrode at different scan rates in a non-Faradic region (1.03~1.13 V vs. RHE). Cdl was determined as the linear slope by plotting anodic current density at 1.08 V against the scan rate (10-100 mV/s)

$$C_{dl} = i_c/v \qquad ECSA = C_{dl}/Cs$$

i_c is the charging current, ν is the scan rate, Cs is the specific capacitance (0.040 mF/cm^2), S is the area of the electrode (1 cm^2).

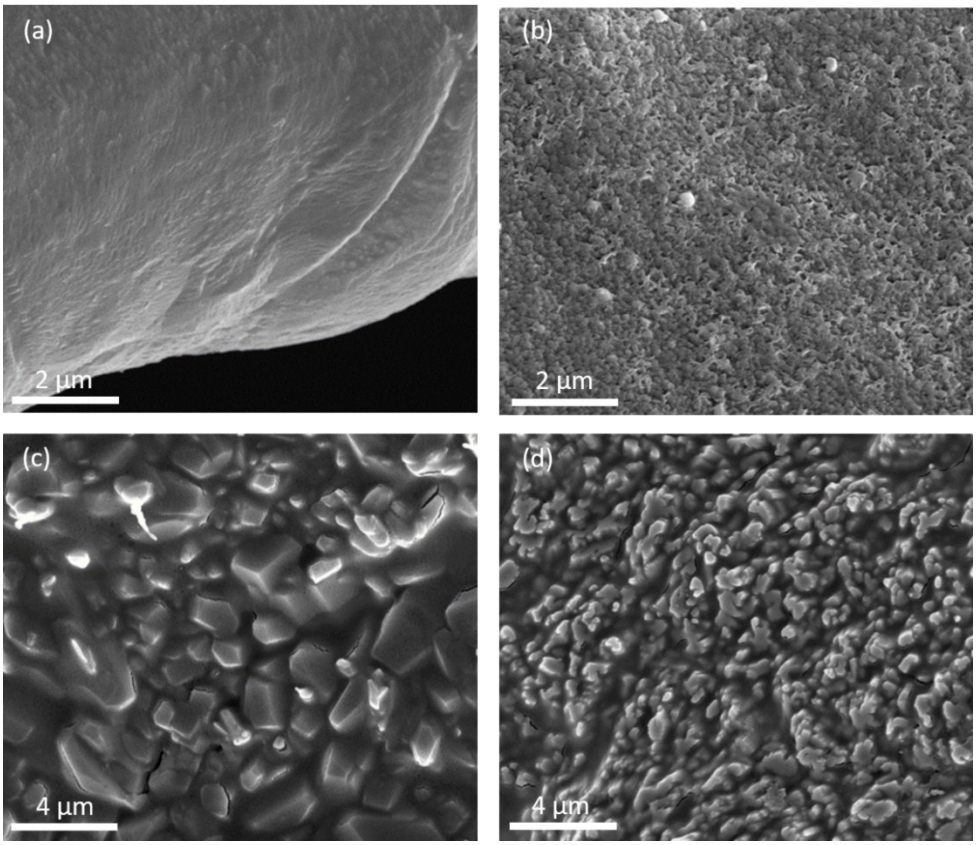

Figure S1. SEM image of the bare NF (a), CeO_2-NF (b), FeP-NF (c) and FeP/CeO_2-NF(d).

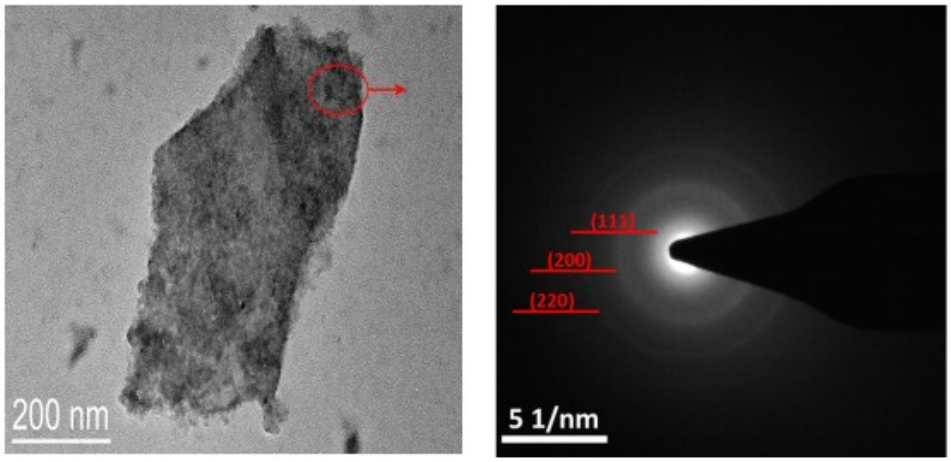

Figure S2. SAED pattern of the FeP/CeO_2-NF electrode.

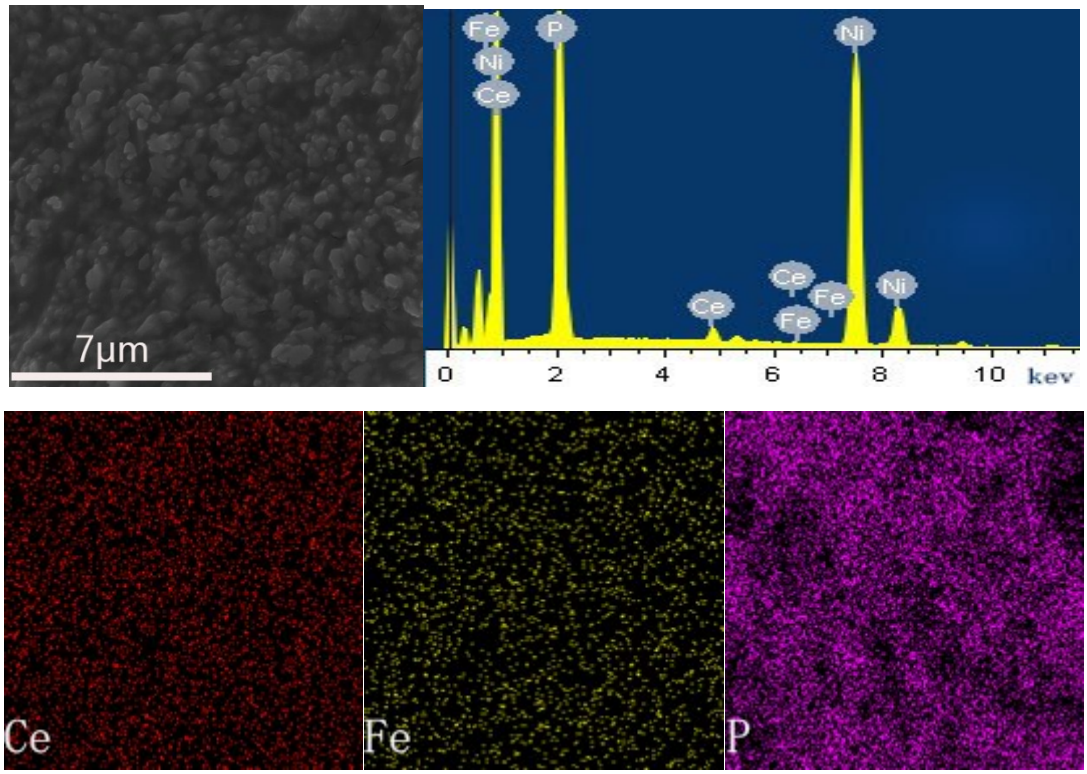

Figure S3. EDX spectra and EDX mapping of the FeP/CeO_2-NF electrode.

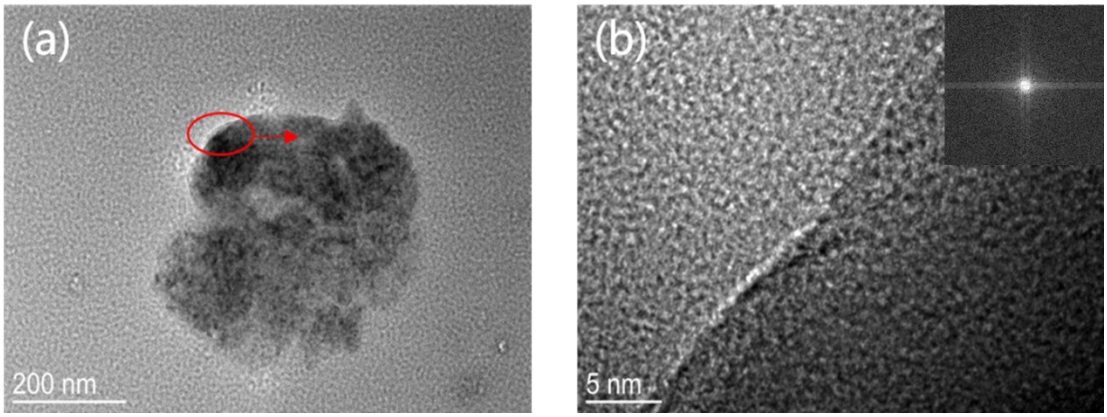

Figure S4. (a and b) TEM and HRTEM images of FeP-NF electrode. Inset in panel b shows the corresponding SAED pattern.

Table S1. Inductively coupled plasma (ICP) analysis of the deposition solution

Solution	Ce(mg/L)
Before deposition	-
After deposition	1.135

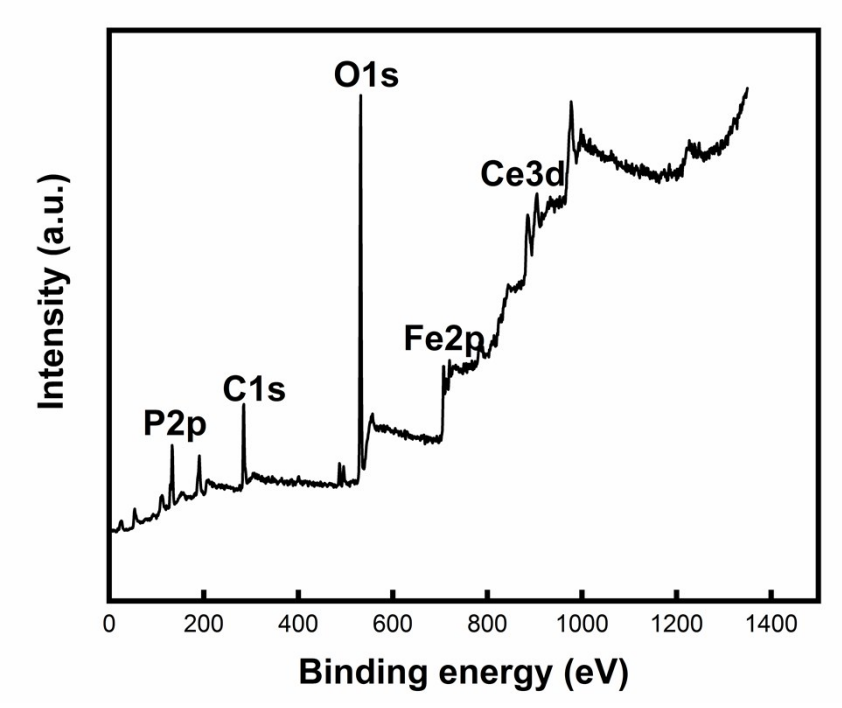

Figure S5. XPS survey spectrum of the FeP/CeO_2-NF electrode before OER.

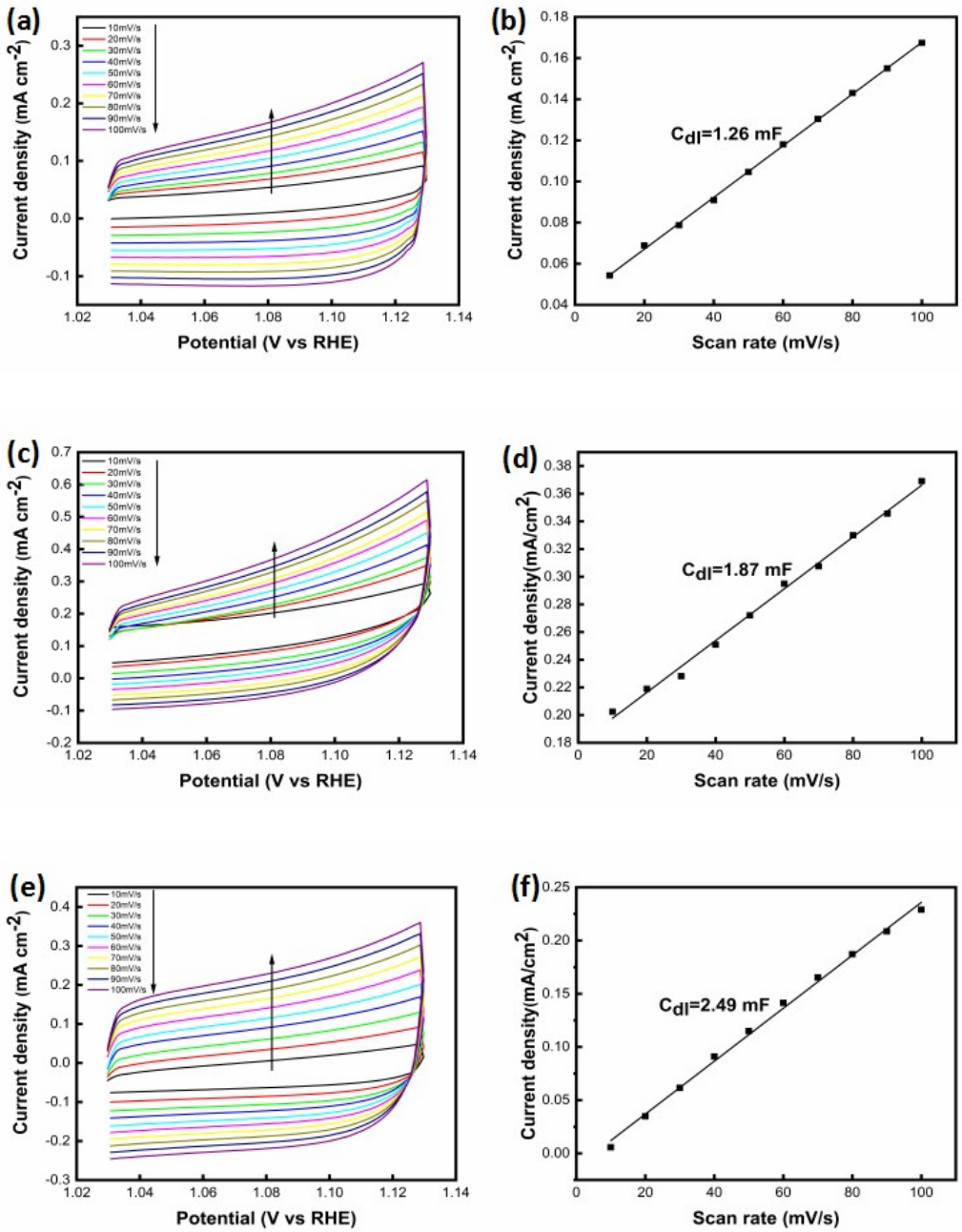

Figure S6. CV curves of CeO_2-NF (a) , FeP-NF (c) and FeP/CeO_2-NF(e) at various scan rates(10 mV/s,20 mV/s,30 mV/s,40 mV/s,50 mV/s,60 mV/s,70 mV/s,80 mV/s,90 mV/s and 100mV/s) in the potential of 1.03-1.13 V and the anodic charging current measured at 1.08 V plotted as a function of scan rate for CeO_2-NF (b) , FeP-NF (d) and FeP/CeO_2-NF(f).

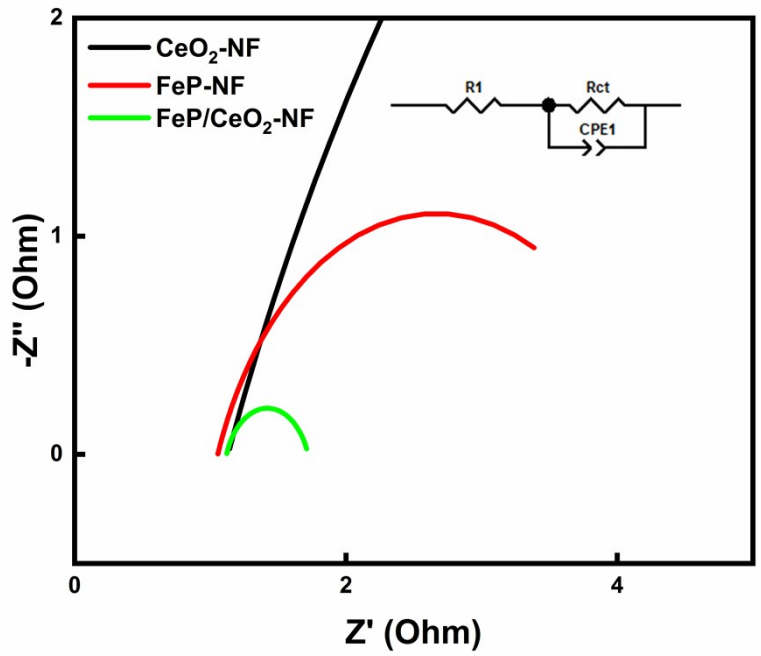

Figure S7. EIS spectra of FeP/CeO_2-NF, FeP-NF and CeO_2.

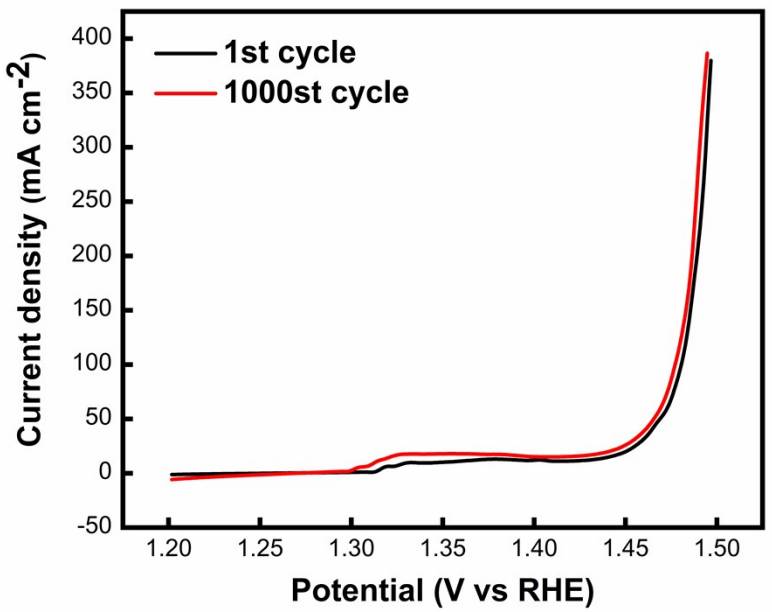

Figure S8. LSV curves before and after 1000 continuous CV cycles.

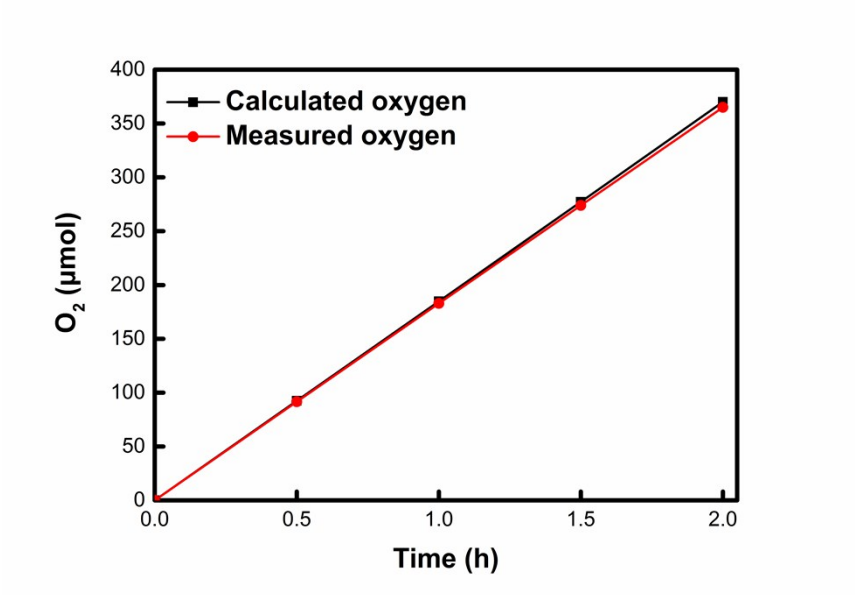

Figure S9. Determination of the Faradicefficiency of the FeP/CeO_2-NF on electrolysis of water at 20 mA/cm^2 in 1.0 M KOH solution.

Table 2. TOF calculated from current density at 20 mA/cm^2

Catalyst	I (mA/cm^2)	Loading (mg)	TOF (s^{-1})
FeP/CeO_2-NF	20	0.28	0.01

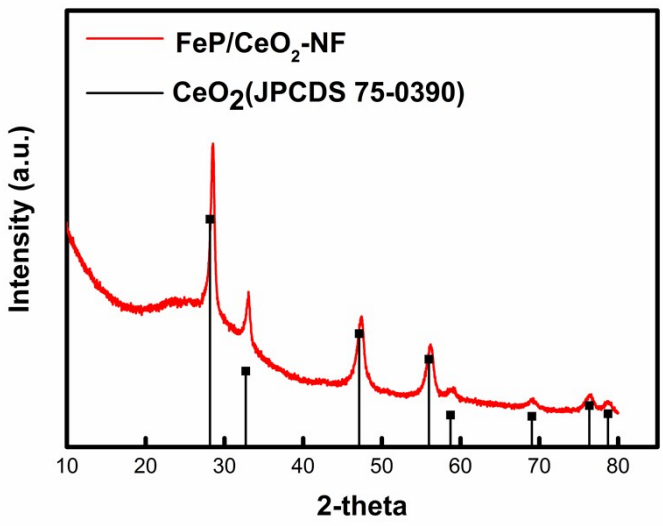

Figure S10. XRD pattern of FeP/CeO_2-NF electrode after OER.

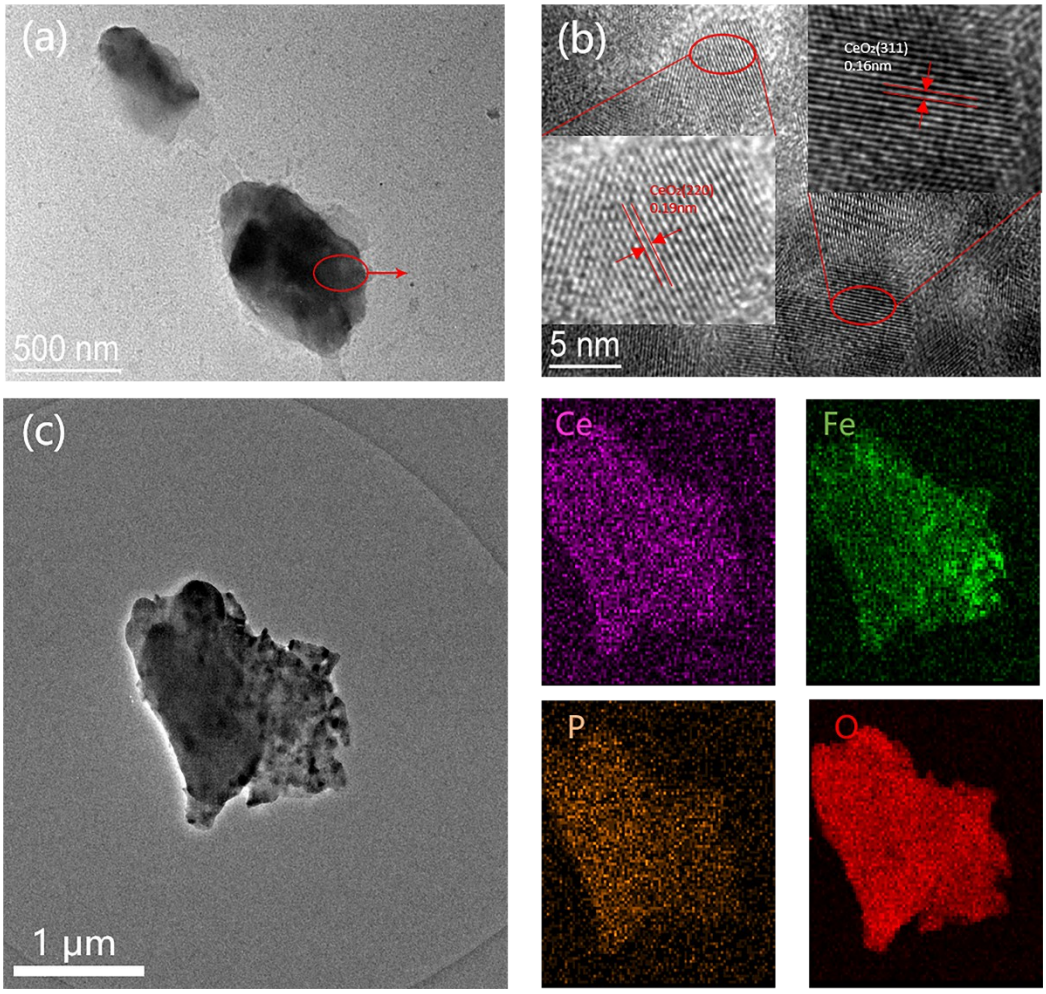

Figure S11. (a and b) The TEM and HRTEM images of FeP/CeO_2-NF electrode after OER; (c) HAADF-STEM image and STEM-EDS element mappings of FeP/CeO_2-NF electrode. Ce pink, Fe green, P yellow, O red.

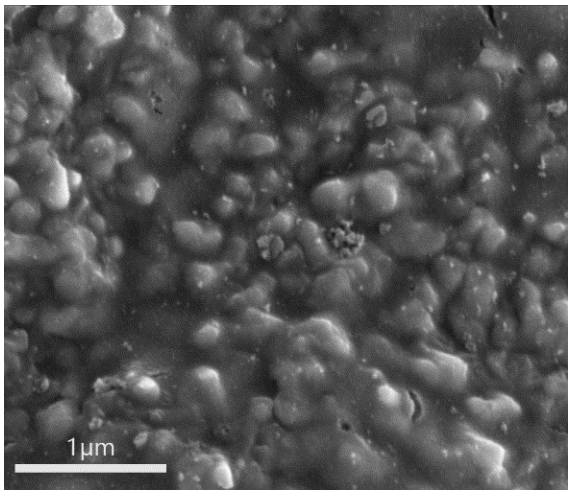

Figure S12. The SEM images of FeP/CeO_2-NF electrode after OER.

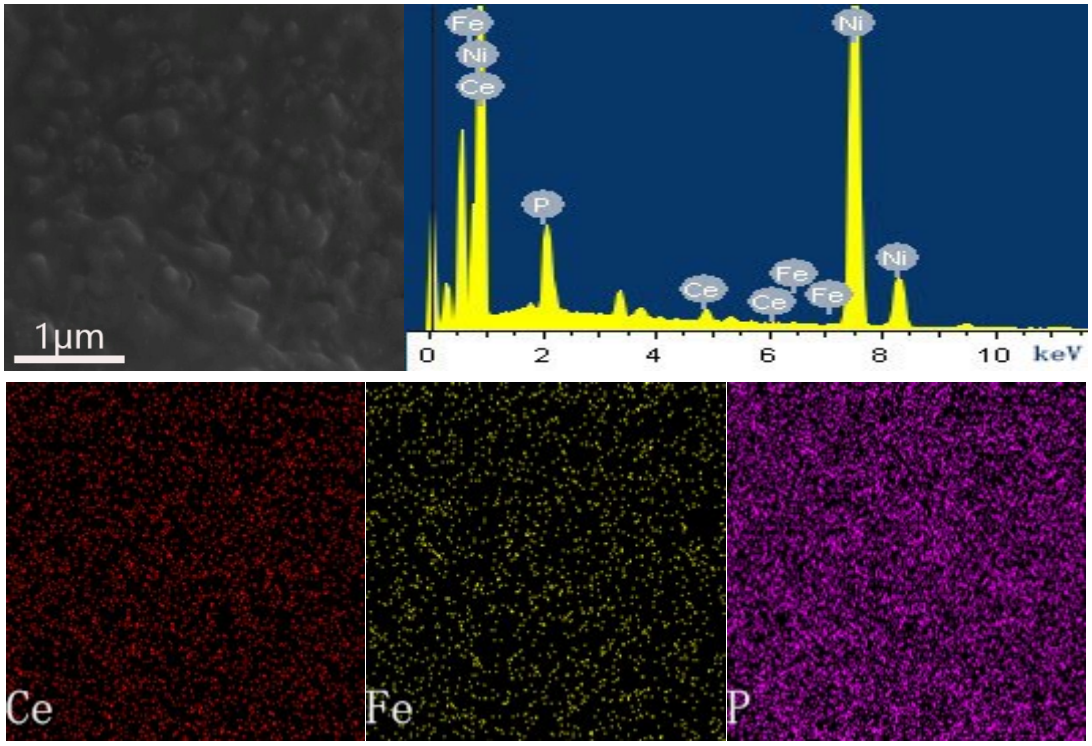

Figure S13. EDX spectra and EDX mapping of the FeP/CeO_2-NF electrode after OER

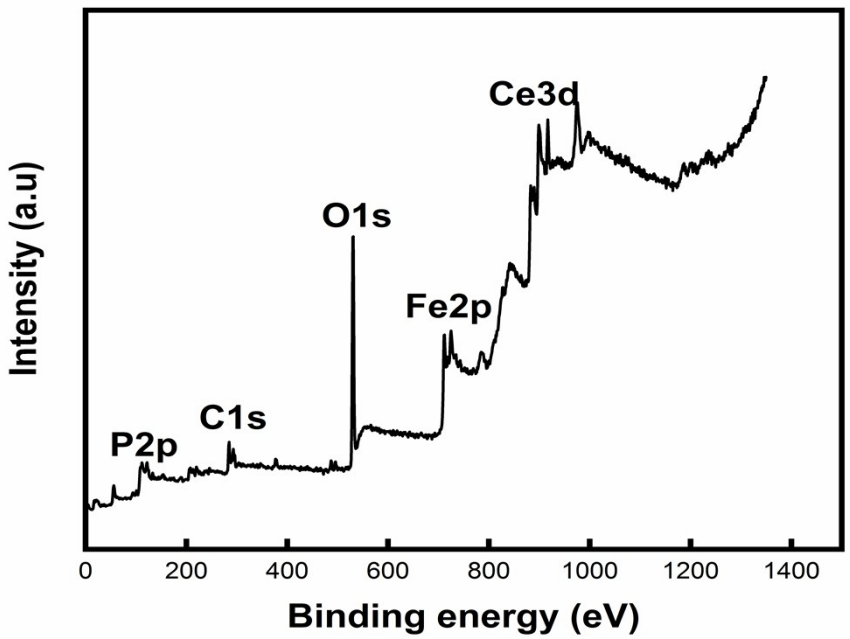

Figure S14. XPS survey spectrum of the FeP/CeO_2-NF electrode after OER.

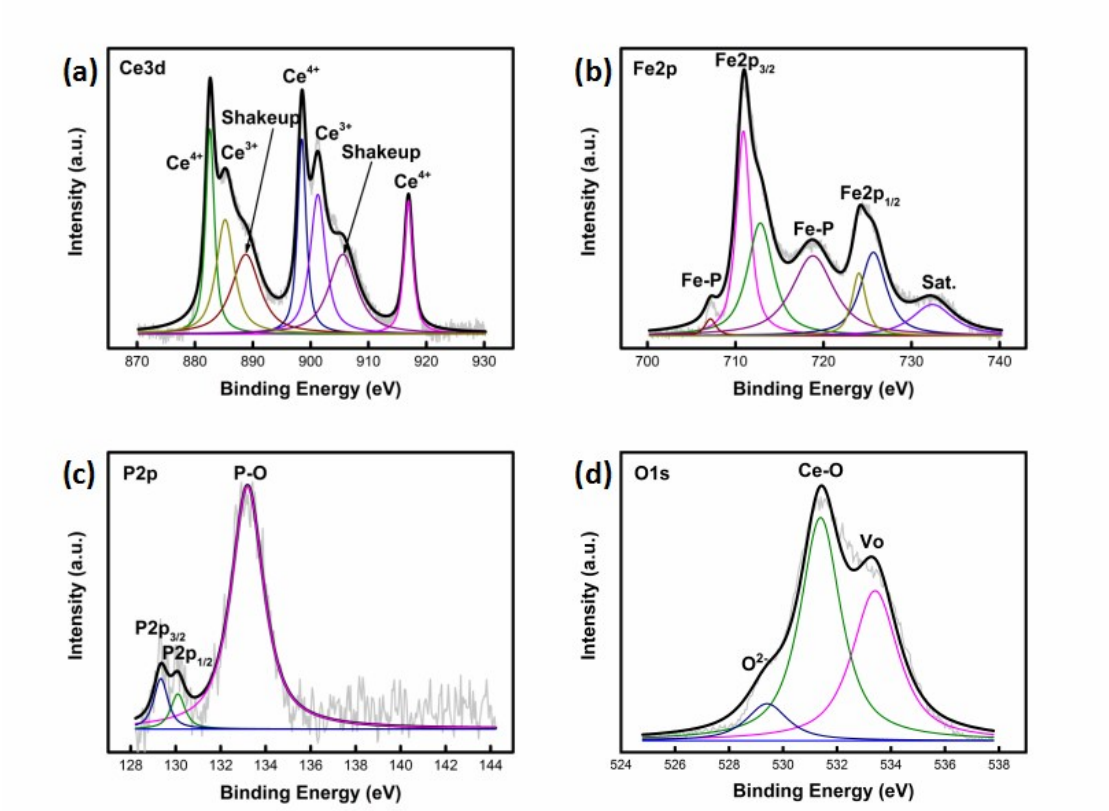

Figure S15. (a) XPS survey spectrum of the FeP/CeO_2-NF electrode and high-resolution XPS spectra of (b) Ce 3d, (c) Fe 2p, (d) P 2p and (e) O 1s after OER.

Table S3. Comparison of the OER performance of FeP/CeO_2-NF with the recently reported catalysts

Electrocatalyst	Electrolyte	I/mA/cm^2	Overpotential η/mV	Tafel slope mV/dec	Refs
FeP/CeO_2-NF	1M KOH	100	245	39.1	This work
NiFeP-NF	1M KOH	100	290	57	1
NiFe(3:1)-P	1M KOH	100	290	42.5	2
FeP-rGO	1M KOH	100	330	49.6	3
FeP NRs@CP	1M KOH	100	413.6	63.6	4
FeP/CoP-CC	1M KOH	100	317	67	5
FeP/NF	1M KOH	100	292	54	6
FeP/Ni_2P NSs	1M KOH	100	285	50.3	7
Ni_4Ce_1@CP	1M KOH	100	330	81.9	8
CeO_2/FeOOH-NF	1M NaOH	100	320	92.3	9
CeO_2/$Ni(OH)_2$/NOSCF	1M KOH	100	450	57	10

(Overpotentials were estimated from the LSV curves presented in the reference literature)

1. J. Yu, G. Cheng and W. Luo, *J. Mater. Chem. A*, 2017, **5**, 11229-11235.
2. P. Li and H. C. Zeng, *J. Mater. Chem. A*, 2018, **6,** 2231-2238.
3. J. Masud, S. Umapathi, N. Ashokaan and M. Nath, *J. Mater. Chem. A*, 2016, **4**, 9750-9754.
4. D. Xiong, X. Wang, W. Li and L. Liu, *Chem. Commun.*, 2016, **52**, 8711-8714.
5. Z. Niu, C. Qiu, J. Jiang and L. Ai, *ACS Sustainable Chem. Eng.*, 2018, **7,** 2335-2342.
6. S. Yao, V. Forstner, P. W. Menezes, C. Panda, S. Mebs, E. M. Zolnhofer, M. E. Miehlich, T. Szilvasi, N. Ashok Kumar, M. Haumann, K. Meyer, H. Grutzmacher and M. Driess, *Chem. Sci.*, 2018, **9**, 8590-8597.
7. Y. Feng, C. Xu, E. Hu, B. Xia, J. Ning, C. Zheng, Y. Zhong, Z. Zhang and Y. Hu, *J. Mater. Chem. A*, 2018, **6**, 14103-14111.
8. D. Zhao, Y. Pi, Q. Shao, Y. Feng, Y. Zhang and X. Huang, *ACS Nano*, 2018, **12**, 6245-6251.
9. J. X. Feng, S. H. Ye, H. Xu, Y. X. Tong and G. R. Li, *Adv. Mater.*, 2016, **28**, 4698-4703.
10. Z. Liu, N. Li, H. Zhao, Y. Zhang, Y. Huang, Z. Yin and Y. Du, *Chem. Sci.*, 2017, **8**, 3211-3217.